A&A 365, L308–L311 (2001)
DOI: 10.1051/0004-6361:20000069

Astronomy & Astrophysics

A high resolution spectroscopic observation of CAL 83 with XMM-Newton/RGS⋆

F. Paerels[1], A. P. Rasmussen[1], H. W. Hartmann[2], J. Heise[2], A. C. Brinkman[2], C. P. de Vries[2], and J. W. den Herder[2]

[1] Columbia Astrophysics Laboratory, Columbia University, 550 West 120th St., New York, NY 10027, USA
[2] SRON Laboratory for Space Research, Sorbonnelaan 2, 3584 CA Utrecht, The Netherlands

Received 3 October 2000 / Accepted 27 October 2000

Abstract. We present the first high resolution photospheric X-ray spectrum of a Supersoft X-ray Source, the famous CAL 83 in the Large Magellanic Cloud. The spectrum was obtained with the Reflection Grating Spectrometer on *XMM-Newton* during the Calibration/Performance Verification phase of the observatory. The spectrum covers the range 20–40 Å at an approximately constant resolution of 0.05 Å, and shows very significant, intricate detail, that is very sensitive to the physical properties of the object. We present the results of an initial investigation of the spectrum, from which we draw the conclusion that the spectral structure is probably dominated by numerous absorption features due to transitions in the L-shells of the mid-Z elements and the M-shell of Fe, in addition to a few strong K-shell features due to CNO.

Key words. stars: atmospheres – stars: individual (CAL 83) – white dwarfs – X-rays: stars

1. Introduction

Supersoft X-ray Sources (or Supersoft Sources, SSS) were among the first new discoveries made with *ROSAT* – in the first PSPC images of the LMC, the SSS stood out immediately (Trümper et al. 1991). In retrospect, some of these objects had been seen before with *Einstein*, but the *ROSAT* detection in short order of several SSS focused attention on them as a class.

It is now generally accepted that the SSS are white dwarf stars undergoing steady nuclear burning in their envelopes. The inferred size of the radiating surface area, coupled with the characteristically very soft optically thick spectra, point to this idea as the natural interpretation for the observed emission. Some SSS are central stars of Planetary Nebulae, or related objects: shell-burning, (mostly) single stars on their way to the white dwarf graveyard. The classical SSS, however, is a high-luminosity ($L \gtrsim 0.1\ L_{\rm Edd}$), soft ($kT \lesssim 50$ eV) low-mass binary with a white dwarf primary. In contrast to the case for neutron stars, for white dwarfs the efficiency of nuclear burning exceeds the efficiency of gravitational energy conversion by accretion, by a factor of order 100, so that SSS can sustain a high luminosity with a sub-Eddington accretion rate.

The basic model for the classical SSS has been worked out by van den Heuvel et al. (1992). A relatively high-mass white dwarf (0.7–1.2 $M_\odot$) can sustain steady nuclear burning of accreted hydrogen near its surface if the accretion rate is in the range 1–4 $10^{-7}\ M_\odot\ {\rm yr}^{-1}$. Such an accretion rate can arise if the mass donor companion star is more massive than the white dwarf (1.5–2.0 $M_\odot$). Mass transfer to the less massive star will cause the binary orbit to shrink, and the donor will transfer mass on a rapid thermal timescale. The predicted luminosities are in the range $6\ 10^{36} - 1\ 10^{38}$ erg s^{-1}, roughly in the observed range for SSS. The binary evolution aspects of this model, including an estimate for the birthrate and prevalence of SSS binaries, have been addressed by Rappaport et al. (1994).

An important part of the interest in the SSS stems from the fact that they may be a significant channel to SN Ia events. Mass is deposited onto the white dwarf at such a high rate that the accreted matter can burn non-eruptively, which makes the white dwarf mass grow (in contrast to low accretion-rate binaries, such as classical novae, which expel most of the previously accreted matter in explosive events), eventually reaching the Chandrasekhar mass. Rappaport et al. (1994) estimate that the rate of Galactic SN Ia supernovae associated with SSS binary evolution could be as high as $\sim$0.006 yr^{-1}.

Send offprint requests to: F. Paerels

⋆ Based on observations obtained with *XMM-Newton*, an ESA science mission with instruments and contributions directly funded by ESA Member States and the USA (NASA).

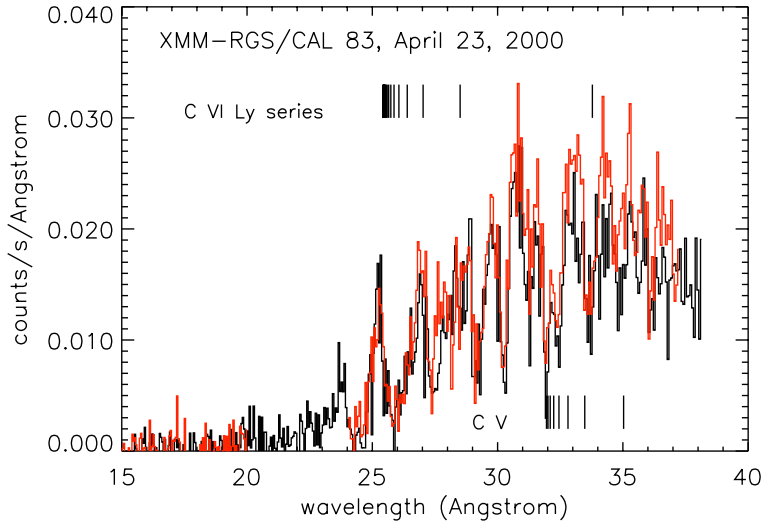

Fig. 1. Exposure corrected, background subtracted spectrum of CAL 83. We show the spectrum measured with RGS 1 (black histogram) overlaid on the spectrum measured with RGS 2 (red histogram), to emphasize the correspondence of coherent features in the spectrum in both spectrometer data sets. The wavelength bin equals 5 original RGS 81 μm CCD spatial bins, which corresponds to approximately 0.06 Å, slightly larger than one resolution element. The range 20.1–23.9 Å is not present in the data from RGS2, because of malfunction of the drive electronics for one CCD chip in this spectrometer. Included for reference are wavelengths of the strongest resonance transitions in hydrogen- and helium-like C

A high resolution soft X-ray spectroscopic observation can in principle directly and definitively settle any remaining doubts about the nature of the emission and the compact object, by detecting characteristic photospheric structure in the spectrum. With a high resolution spectrum, we can attempt to obtain an accurate estimate for the fundamental stellar and binary parameters (luminosity, effective temperature, radius and mass of the white dwarf, mass transfer rate), which has a direct bearing on the evolutionary status and ultimate fate of the binary. In this *Letter*, we present preliminary results of a high resolution spectroscopic observation of the important SSS CAL 83 (Cowley et al. 1984; Pakull et al. 1985; Crampton et al. 1987; Smale et al. 1988; Parmar et al. 1998) which directly addresses the above issues.

2. Data analysis

CAL 83 was observed by *XMM-Newton* (Jansen et al. 2001) during the Calibration/Performance Verification phase of the observatory, on April 23, 2000, for a total of 45.1 ksec. Data was obtained with both the Reflection Grating Spectrometers (RGS, den Herder et al. 2001) and the EPIC focal plane imaging cameras (Turner et al. 2001). For the purpose of this paper, the high resolution spectrum obtained with RGS holds the primary interest, and we will only discuss the RGS data.

The data were processed using custom software originally developed for the analysis of RGS ground calibration data, which is nearly identical in function to the RGS branch of the Science Analysis System (SAS). Telemetered CCD events are read in frame by frame and are offset–corrected on a pixel by pixel basis using median readout maps, compiled from about 40 diagnostic images (den Herder et al. 2001) per CCD chip, those available from the ten most recent revolutions (20 days). This process nearly eliminates flickering pixels from the dataset. Remaining flickering and warm pixels are removed from the datasets by thresholding duty cycle maps (for each CCD), also generated from about 10 contemporaneous revolutions. Gain and CTI correction are performed to align the signal/energy scale across all CCD readouts. Then, event reconstruction is performed on a frame–by–frame basis where connected pixels containing significant signal are recombined into composite events and the composite event signal is calculated from the sum of individual (corrected) signals.

The standard event grade combination comprises events which fall within a 2×2 pixel region, where two pixels diagonally opposed to one another within the 2×2 region are considered two separate events. The event coordinates are mapped into focal plane two–dimensional angular coordinates (dispersion and cross–dispersion). The dispersion coordinates are based on the known geometry of the RGS combined with a preliminary in–flight calibration based on the emission line spectra of HR 1099 and Capella which self–consistently determined the instrumental boresight relative to the star tracker. The event positions are corrected for small drifts in aspect.

Events are then windowed in the dispersion–pulseheight and focal planes, using optimum extraction masks utilized by the response matrix generator. Background subtraction was performed using background sampling regions on either side (in the cross–dispersion direction) of the source illuminated region. Finally, a spectrum file was created by histogramming the corrected countrates in each dispersion channel. A response generator was used to produce an observation specific

response matrix that provided an array of nominal wavelength/energy values corresponding to each channel in the spectrum file. This procedure was performed for both the first and second orders for each spectrometer, but only the first order spectra contained significant data.

Figure 1 shows the exposure-corrected, background subtracted spectrum from RGS 1 and 2.

We show the spectrum obtained with the two separate spectrometers superimposed, in order to emphasize that most of the observed spectral detail is real, since it appears in both instruments. It is immediately obvious from a glance at Fig. 1 that blackbody spectral models, or indeed any smooth continuum spectrum, is completely inadequate to characterize the spectrum of CAL 83, and, by extrapolation, SSS in general. Previous low-resolution studies with *ROSAT* (Greiner et al. 1991; see also Heise et al. 1994) and *BeppoSAX* (Parmar et al. 1998) yielded circumstantial evidence that the spectrum had to deviate from a simple blackbody (the bolometric correction associated with a blackbody yields estimates for the total luminosity that exceed the Eddington limit by a large factor), but the spectral structure that must be present in any real stellar photospheric spectrum is seen here for the first time.

We have indicated the wavelengths of the strongest resonance lines in the H- and He-like ions of C in Fig. 1. At the approximate densities and temperatures in the atmosphere (corresponding to $kT \sim 50$ eV, $\log g \sim 8.5$), CNO are expected to be primarily in their H- and He-like charge states, and one might expect to see their absorption lines in the spectrum because of their high abundances. Indeed, at first sight, both C VI Lyα (33.73 Å) and the C V λ34.97 Å $n = 1$–3 resonance line appear to line up with a strong absorption feature in the spectrum. Both the C VI Ly series limit, and the C V ionization limit similarly coincide with a strong feature. However, there is no such correspondence for any of the wavelengths in N. Also, closer inspection reveals the presence of other deep absorption features (e.g. the ones at 30.5 Å, 29.0 Å) that do not correspond to any transitions in the H- and He-like ions of C, N, or O.

We illustrate this finding in the top panel of Fig. 2, which shows the average of the two spectra from RGS 1 and 2, compared to a model atmospheres spectrum calculated for a hydrogen atmosphere at $kT_{\rm eff} = 45$ eV, $\log g = 8.5$, with trace amounts of CNO added at their LMC abundance levels. This, and other models to be discussed in this paper, have been calculated with Hubený's atmospheres code TLUSTY (Hubený 1988; Hubený & Lanz 1995), as applied to the conditions in white dwarfs (Hartmann & Heise 1997; Hartmann et al. 1999). We added absorption by neutral gas, of column density $N_{\rm H} = 6.5\ 10^{20}$ cm^{-2} (Gänsicke et al. 1998), and convolved the model with the response of the RGS. Clearly, this CNO dominated spectrum does not have the dense absorption structure we see in CAL 83.

In our next attempt at interpretation of the spectral structure, we calculated a small grid of models around

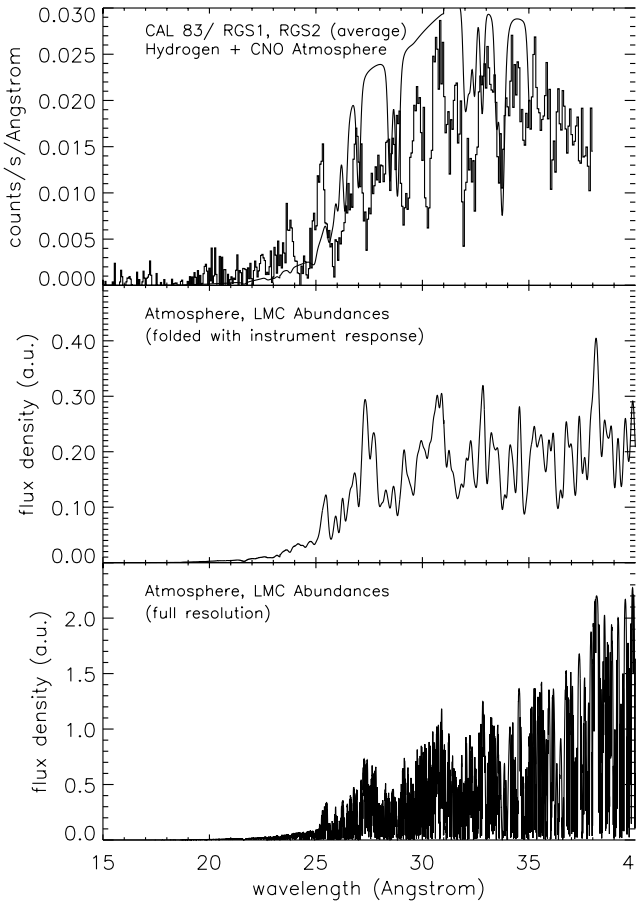

Fig. 2. *Top panel*: average spectrum of CAL 83 (average of RGS1 and RGS2). Superimposed is a model atmospheres spectrum calculated for $kT_{\rm eff} = 45$ eV, $\log g = 8.5$, H + CNO (LMC abundances). The spectrum of CAL 83 clearly has a richer spectrum than this H+CNO atmosphere. *Middle panel*: same atmosphere, with the abundant elements Ne-Ca and Fe added (LMC abundances); the spectrum has been convolved with the RGS instrument response. This spectrum qualitatively resembles the data. *Lower panel*: the same spectrum, but at the full resolution of the model calculation. The structure observed with the RGS is evidently not resolved

$kT_{\rm eff} = 45$ eV, $\log g = 8.5$, this time with all abundant elements up to Fe, at their LMC abundance levels. These spectra all indeed bear a qualitative resemblance to the spectrum of CAL 83. An example (again at $kT_{\rm eff} = 45$ eV, $\log g = 8.5$) is shown in the middle panel of Fig. 2. The spectrum has been convolved with the instrument response. The general structure of the model appears similar to the spectrum of CAL 83. But most of the structure visible in this model is not due to isolated, strong absorption lines, but instead is due to large numbers of closely spaced, narrow absorption features from transitions in the L shells of Ne through Ca, as well as Fe M shell transitions. This dense forest of transitions is actually not resolved by the RGS, as is illustrated by the bottom panel in Fig. 2, where we show the same model as in the middle panel, but before convolution with the instrument response.

We did not attempt a formal fit of these models to the measured spectrum. Even though their qualitative appearance matches the shape of the spectrum, they all differ from the data in significant details. In a general sense, the fact that the discrete absorption spectrum has not been resolved implies that we do not have the most powerful spectroscopic diagnostics that would result from the presence of a few isolated strong transitions in single ions. The dependence of the shape and strength of these features on the properties of the atmosphere (mainly density and temperature) would have given us unambigous estimates of the stellar parameters. Instead, the sensitivity comes about through a dependence of the ionization balance of the mid-Z elements and Fe on temperature and density, and this diagnostic is of course directly subject to uncertainties in the chemical composition of the photosphere. The interpretation may also be sensitive to the computational treatment of the problem and the completeness and accuracy of the atomic structure data used to calculate the line opacities, as well as to uncertainties in the treatment of collisional broadening of the absorption lines. We will address these issues in a future paper.

3. Conclusions

We have presented the first high resolution X-ray spectrum of CAL 83. With *XMM-Newton* RGS, we finally conclusively demonstrate the photospheric origin of the soft X-ray emission. Moreover, our spectrum qualitatively resembles the spectrum expected for the emission from a very hot white dwarf star, and therefore confirms the basic model for binary Supersoft X-ray Sources.

We detect radiation from the photosphere between 20 and ∼40 Å, at an approximately constant wavelength resolution of 0.05 Å. The spectrum shows very significant absorption structure. From comparison to model atmospheres calculations at $kT_{\rm eff} \sim 45$ eV, $\log g \sim 8.5$, for varying abundances, we conclude that most of this structure is due to the superposition of numerous, unresolved narrow absorption features due to transitions in the L shells of the mid-Z elements, the M shell of Fe, as well as in the K shell of C. A quantitatively reliable estimate of the stellar parameters has to await a detailed analysis in terms of a series of dedicated model atmospheres calculations.

Acknowledgements. The Columbia University group is supported by the US National Aeronautics and Space Administration. The Laboratory for Space Research Utrecht is financially supported by NWO, The Netherlands Organization for Scientific Research.

References

Cowley, A. P., Crampton, D., Hutchings, J. B, et al. 1984, ApJ, 286, 196
Crampton, D., Cowley, A. D., & Hutchings, J. B. 1987, ApJ, 321, 745
den Herder, J. W., Brinkman, A. C., Kahn, S. M., et al. 2001, A&A, 365, L7
Gänsicke, B. T., van Teeseling, A., Beuermann, K., & de Martino, D. 1998, A&A, 333, 163
Greiner, J., Hasinger, G., & Kahabka, P. 1991, A&A, 246, L17
Hartmann, H. W., & Heise, J. 1997, A&A, 322, 591
Hartmann, H. W., Heise, J., Kahabka, P., Motch, C., & Parmar, A. N. 1999, A&A, 346, 125
Heise, J., van Teeseling, A., & Kahabka, P. 1994, A&A, 288, L45
Hubený, I. 1988, Comput. Phys. Commun., 52, 103
Hubený, I., & Lanz, T. 1995, ApJ, 439, 875
Jansen, F., Lumb, D., Altieri, B., et al. 2001, A&A, 365, L1
Pakull, M., Ilovaisky, S. A., & Chevalier, C. 1985, Space Sci. Rev., 40, 229
Parmar, A. N., Kahabka, P., Hartmann, H. W., Heise, J., & Taylor, B. G. 1998, A&A, 332, 199
Rappaport, S. A., di Stefano, R., & Smith, J. D. 1994, ApJ, 426, 692
Smale, A. P., et al. 1988, MNRAS, 233, 51
Trümper, J., Hasinger, G., Aschenbach, B., Bräuniger, H., & Briel, U. 1991, Nat, 349, 579
Turner, M. J. L., Abbey, A., Arnaud, M., et al. 2001, A&A, 365, L27
van den Heuvel, E. P. J., Bhattacharya, D., Nomoto, K., & Rappaport, S. A. 1992, A&A, 262, 97